Integrated Transcriptomic Profiling of Metabolic Alterations in Breast and Ovarian Cancer

Muskaan Dimri[1], Shalini Mani*[1]

[1]*Department of Biotechnology, Jaypee Institute of Information Technology, Noida, India-201309*

muskaandimri@gmail.com, *shalini.mani@jiit.ac.in*

Abstract

Extensive metabolic reprogramming that supports increased energy demand, biosynthesis, and tumor cell survival is closely linked to the progression of cancer. Key dysregulated metabolic pathways and genes across breast and ovarian cancers were identified in this study using a metabolism-centric integrative bioinformatics approach. First, a 434-node protein–protein interaction (PPI) network was created using dysregulated metabolic pathways found in cancer. The top 10 hub genes were selected based on degree centrality after network topological analysis was carried out using CytoHubba, indicating their possible regulatory significance within metabolic networks. The biological significance of the chosen hub genes was confirmed by functional enrichment analysis using g: Profiler, which showed a significant enrichment of pathways linked to energy metabolism, oxidative phosphorylation, and mitochondrial function.

Expression profiling of the shortlisted genes was carried out across six separate GEO datasets that included tumor and normal samples, including two ovarian cancer datasets and three breast cancer datasets, in order to further validate these findings. Hub genes were uniformly dysregulated in all types of cancers, and the tumor samples exhibited varying expression patterns to the normal tissues. The significant dysregulation of the hub genes in tumor conditions was verified by the differential expression analysis and the high correlation among them in normal samples and dysregulated pattern in tumor samples by the co-expression analysis. Principal component analysis (PCA) also showed strong separation between tumor and normal samples as a result of the expression of these genes and the combined effect of these genes in cancer-related metabolic alterations in patient samples of ovarian and breast cancer. The whole scenario is that this integrative analysis has significant metabolic hub genes that are systematically dysregulated in both the ovarian and breast cancers, which provides mechanistic understanding of cancer metabolism and a viable platform upon which to conduct further functional and therapeutic studies.

Keywords:
Cancer metabolism; Metabolic reprogramming; Hub genes; CytoHubba; mitochondrial dysfunction; Oxidative phosphorylation

1. Introduction

Cancer has since stayed a health problem in the world with increasing incidences reported to be approximately 20 million in 2022 with approximately 9.7 million deaths worldwide based on GLOBOCAN database [1]. The most frequently diagnosed cancer is breast cancer which annually affects more than 2.3 million women all over the globe. On the contrary, the most fatal gynaecological condition is ovarian cancer that kills over 3,13,000 women and over 2,07,000 people per year worldwide in ways of new infections and deaths respectively. The disease has high mortality rate owing in part to the fact that the disease is commonly detected in its metastatic stages, there are no good screening biomarkers and the disease is asymptomatic in its early stages [2]. Metastatic breast cancer has a 5-year survival of approximately 28% and advanced-stage ovarian cancer still has an approximate survival rate of about 30%, notwithstanding the advancement in therapeutic methods. This underscores the necessity to have improved molecular classification and therapeutic targets [3].

The characteristic of cancer development is metabolic reprogramming that allows tumor cells to keep their rapid proliferation, evade apoptosis, and adapt to altering microenvironmental parameters. Even though aerobic glycolysis was elucidated by the classical Warburg effect as the major metabolic phenotype in tumors, emerging studies indicate that nevertheless mitochondrial activity remains highly active and core in a high percentage of cancers [4-5]. Increased mitochondrial respiratory capacity has been particularly linked to the aggressiveness of tumors, chances of metastasis, and resistance to any treatment in particular in ovarian and breast malignancies. Recent extensive transcriptome and proteomic studies show that more than 40-60% of solid tumors are hyper-expressed with oxidative phosphorylation (OXPHOS) genes [6-7]. Tumor metabolism requires mitochondrial metabolic activities, such as oxidative phosphorylation, tricarboxylic acid cycle, fatty acid 2 -oxidation, amino acid metabolism, mitochondrial translation, respiratory electron transport, mitochondrial biogenesis, and ROS detoxification. Mitochondrial dysfunctions cause cellular signalling pathway disruption, ATP metabolism, redox balance, and oncometabolites [8].

Noteworthy, to date, malignancies with high OXPHOS activity have been found to have a higher biomass and ATP producing rate of mitochondria that is 2-3 times higher. These cells are more susceptible to mitochondrial-targeted therapies which is because they are more reliant on the integrity of the electron transport chain [9]. Single-gene studies cannot explain cancer-related changes on the basis of system-wide metabolic alterations in the mitochondria due to the complexity of mitochondrial metabolism. Combination of patient-derived transcriptomic data and mitochondrial network reconstruction provides a system level framework in analyzing the metabolic weaknesses in ovarian and breast cancer [10].

This research offers a basis on how mitochondrial signature markers can be used in different malignancies to create biomarker-based metabolic classifications and the applicability of mitochondrial network dynamics in solid malignancies. The applicability of such techniques to other forms of cancer that can exhibit metabolic heterogeneity can help advance further the emergence of precision oncology therapy that directly addresses tumor bioenergetics.

2. Materials & Methods

2.1. Datasets

The validation of the associated mitochondrial metabolic pathway-derived hub genes in BC and OVC identified through network analysis was done using publicly available gene expression datasets- retrieved from the NCBI Gene Expression Omnibus (GEO) database [11]. A total of six independent datasets were included in this study, comprising three breast cancer datasets (GSE10810, GSE42568, and GSE29431) and two ovarian cancer datasets (GSE14407 and GSE18520) were analysed in R Programme.

These datasets enabled a holistic comparative case-control analysis for the validation of hub genes. The datasets consisted of gene expression profiles derived from tumor and corresponding normal tissue samples. All selected datasets were generated using well-annotated microarray platforms GPL570 (Affymetrix Human Genome U133

Plus 2.0 Array) and included sufficient sample size and complete experimental metadata to ensure statistical robustness. The inclusion of multiple independent datasets minimized dataset-specific bias and enhanced the reproducibility and generalizability of the findings across hormone-driven malignancies. The use of multiple independent breast and ovarian cancer datasets allowed for cross-validation of pathway-derived hub genes.

Detailed information regarding sample composition, platform type, and experimental design for each dataset is provided in Table 1.

Table 1: Summary of Gene Expression Omnibus (GEO) datasets included in the study.

Sno.	Dataset ID	Cancer Type	Platform	Normal Samples (n)	Tumor Samples (n)	Experimental Design
1	GSE18520	Ovarian cancer	GPL570	10	53	Case–control gene expression profiling of normal ovary and ovarian tumor tissues
2	GSE14407	Ovarian cancer	GPL570	12	12	Comparative transcriptomic analysis between normal ovarian tissue and ovarian cancer samples
3	GSE29431	Breast cancer	GPL570	12	54	Balanced case–control design for breast cancer expression analysis
4	GSE42568	Breast cancer	GPL570	17	104	Large-scale expression profiling of normal breast tissue and breast tumors
5	GSE10810	Breast cancer	GPL570	27	31	Differential gene expression analysis between normal breast samples and breast cancer tissues

2.2. Methods and Tools

The methodology followed in this study is illustrated in the Figure 1.

2.2.1. Selection of mitochondrial metabolic pathways and gene extraction

An investigation into the involvement of mitochondrial metabolic abnormalities in breast and ovarian cancer used an analytical approach centered upon pathways. Eight large mitochondrial metabolic pathways – oxidative phosphorylation (OXPHOS), pentose phosphate pathway (PPP), glutaminolysis, fatty acid oxidation, production of nucleotides through biosynthesis, one-carbon metabolism, lipid metabolism, and glycolysis – were chosen as having a well-established role in the development of malignancies according to pathway databases such as REACTOME, KEGG and scientific literature [12] [13]. A total of 434 genes associated with the eight pathways were combined to create a gene set that was subsequently utilized to develop a protein-protein interaction network.

2.2.2. Protein–protein interaction network construction

To examine protein–protein interactions (PPIs), the STRING database was utilized [14]. After uploading the curated list of genes associated with mitochondrial metabolism to STRING, interactions supported by co-expression, curated databases, experimental data, and computer predictions were returned. The high-confidence interaction score criterion was applied to ensure the network's dependability. In order to view the interaction network and perform additional topological analysis, it was first exported and then imported into Cytoscape [15].

2.2.3. Network analysis and hub gene identification

Cytoscape was used to do a topological analysis of the PPI network. The cytoHubba plugin, which ranks nodes according to network centrality metrics, was used to identify hub genes. The main ranking criterion for identifying highly linked and functionally significant genes was degree centrality. The top-ranked genes were chosen for functional enrichment and expression validation analyses because they were regarded as hub genes.

2.2.4. Functional enrichment analysis

The identified hub genes were subjected to functional enrichment analysis was done via various tools like via g: Profiler [16], DAVID [17], Shinygo [18] in order to clarify their biological importance. Using common enrichment methods, Gene Ontology (GO) and pathway enrichment analyses were carried out. False discovery rate (FDR)–adjusted p-values < 0.05 were used to filter enriched keywords and pathways, with an emphasis on energy metabolism, oxidative phosphorylation, and mitochondrial respiratory activities. The enrichment analysis was visualised using R Programme packages like ggplots.

2.2.5. Expression validation using GEO dataset

Publicly available gene expression datasets were selected from the Gene Expression Omnibus (GEO) database. According to the original dataset annotations, the datasets for ovarian cancer (GSE14407 and GSE18520) and breast cancer (GSE10810, GSE42568, and GSE29431) were selected based on the availability of tumor and normal samples. All preprocessing and statistical analyses were conducted in the R programming environment (version 4.5.2; R Foundation for Statistical Computing, Vienna, Austria). The GEOquery software was used to obtain GEO datasets, and Biobase was used to maintain ExpressionSet objects. Using platform-specific annotation software (hgu133plus2.db and AnnotationDbi), probe identifiers were mapped to official gene symbols. The probe with the lowest adjusted p-value was retained when multiple probes matched a single gene.. The limma package was used to perform a differential gene expression analysis between tumor and normal samples. Linear models were fitted (lmFit) and then empirical Bayes moderation (eBayes) was applied; genes with $|\log_2 \text{fold change}| \geq 1$ and an adjusted p-value ≤ 0.05 were deemed to be significantly differentially expressed. Global transcriptome variation was assessed using principal component analysis (PCA) with base R's prcomp function. Pearson correlation coefficients (cor function) were used to assess gene-gene co-expression among hub genes independently for tumor and normal samples. Correlation shift analysis was used to investigate variations in the strength of co-expression between conditions, and pheatmap was used to visualize correlation matrices. For publication-quality presentation, all graphical outputs, such as PCA plots, volcano plots, lollipop plots, correlation density plots, and heatmaps, were created with ggplot2 and pheatmap.

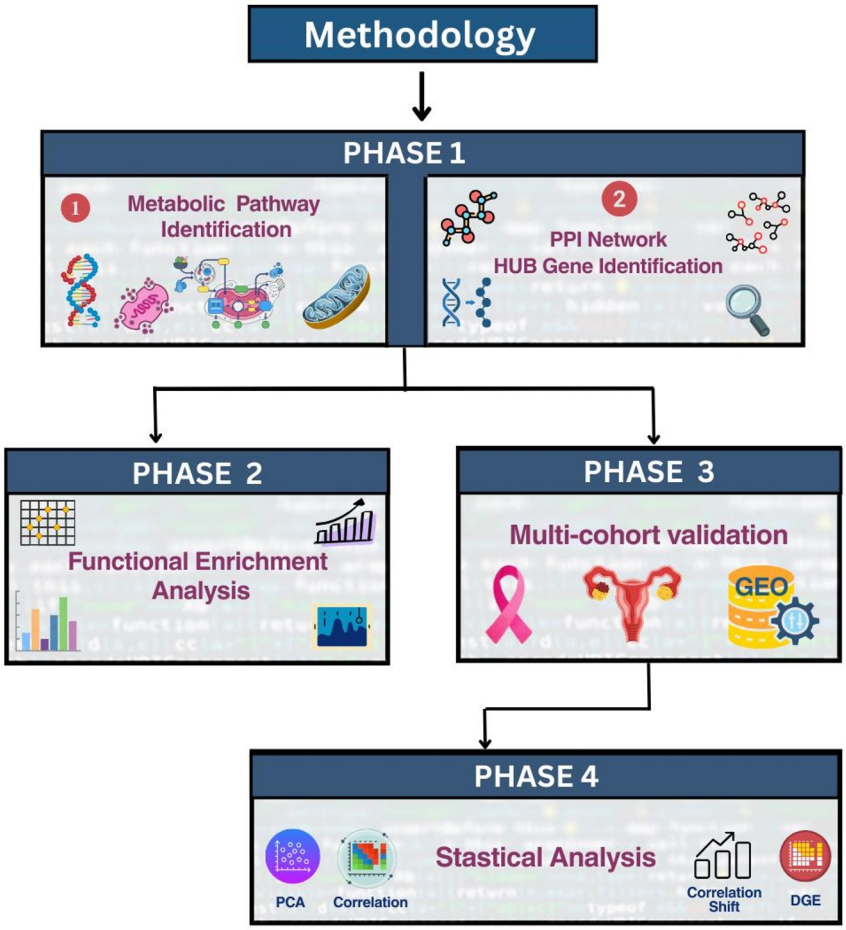

Fig. 1- Schematic overview of the study methodology. Phase 1 involved metabolic pathway identification followed by protein–protein interaction (PPI) network construction to determine hub genes. Phase 2 included functional enrichment analysis of the identified hubs. Phase 3 comprised multi-cohort validation using independent GEO datasets. Phase 4 involved statistical analyses, including principal component analysis (PCA), gene–gene correlation analysis, correlation shift assessment, and differential gene expression (DGE) analysis.

3. Results

3.1 PPI-Based Hub Gene Identification

Using the STRING database, genes from specific cancer-relevant metabolic pathways were incorporated into a 435-node protein–protein interaction (PPI) network in order to identify important regulatory elements driving cancer-associated mitochondrial metabolic reprogramming. Extensive interconnectedness was demonstrated by the built network, indicating coordinated regulation of many metabolic processes.

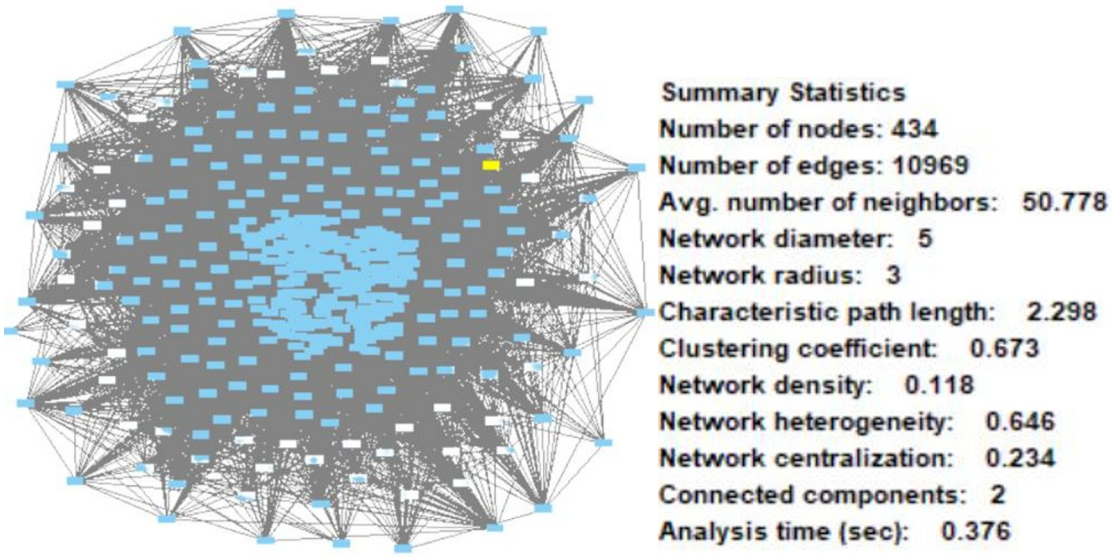

Fig. 2- Protein–protein interaction network of the Mitochondrial metabolic pathways demonstrating extensive interconnectivity.

Highly linked nodes were ranked using a degree-based approach using the Cytohubba plugin. Notably, NDUFS2, NDUFS3, NDUFS8, NDUFV1, NDUFA9, NDUFAB1, SDHA, SDHB, UQCRC1, and GAPDH were among the top-ranked hub genes. These genes operate in different but related metabolic processes. Core subunits of Mitochondrial Complex I (NADH: ubiquinone oxidoreductase) include NDUFS2, NDUFS3, NDUFS8, NDUFV1, NDUFA9, and NDUFAB1 [19] [20] [21]. They participate in electron transfer from NADH to ubiquinone, which starts the mitochondrial electron transport chain (ETC). SDHA and SDHB are catalytic subunits of Mitochondrial Complex II (succinate dehydrogenase), functioning at the intersection of the tricarboxylic acid (TCA) cycle and the ETC by oxidizing succinate to fumarate while transferring electrons to ubiquinone [22] [23]. UQCRC1 is a structural component of Mitochondrial Complex III (cytochrome bc1 complex), facilitating electron transfer from ubiquinol to cytochrome c [24] [25]. In contrast, GAPDH (glyceraldehyde-3-phosphate dehydrogenase) is a key cytosolic enzyme of glycolysis, catalyzing the conversion of glyceraldehyde-3-phosphate to 1,3-bisphosphoglycerate, and is frequently implicated in metabolic reprogramming in cancer [26] [27]. All of these hub genes are tightly connected to mitochondrial bioenergetics.

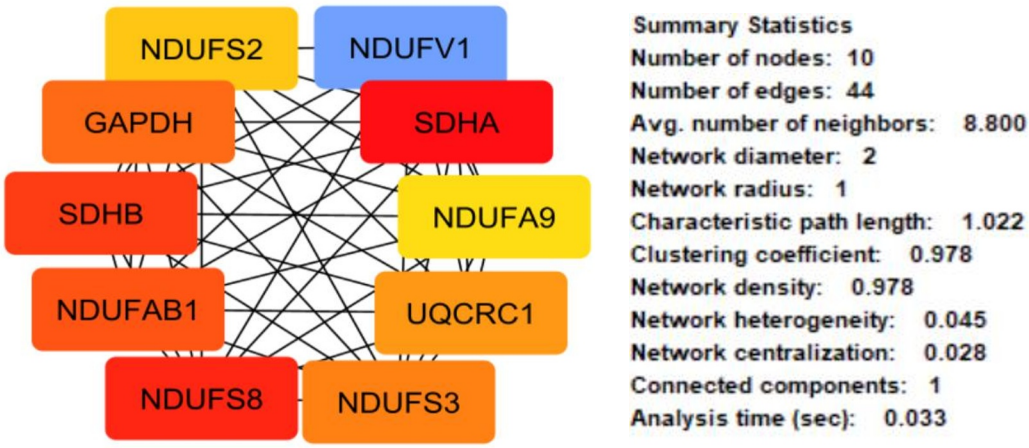

Fig. 3: Protein–protein interaction network of the selected metabolic hub genes demonstrating extensive interconnectivity (10 nodes, 44 edges) and strong clustering, highlighting a tightly coordinated module.

3.2 Functional Enrichment

Functional enrichment performed helped in the further validation enrichment of the hub gene via Gene Ontology (GO), Biological Process (BP), Cellular Component (CC), and Molecular Function (MF). These genes were shown to be very highly enriched in processes that involved mitochondrial oxidative phosphorylation. High gene ratios (~0.8 -1.0) and significant Padj between (3.0 -10 $^{-8}$ and 3.0 -10^{-7}) of the hub genes showed them enriched in aerobic respiration, cellular respiration, cellular respiration and aerobic ETC in the Biological Process Mitochondrial ATP synthesis also became enriched by proton motive force, which is indicative of a coordinated role in electron transport and ATP synthesis [28] [29]. The respiratory chain complex, respiratory chain complex I, NADH dehydrogenase complex and oxidoreductase complex were significantly enriched in the Cellular Component category with adjusted p-values between the range of 1.0 × 10 -5 to 1.0 × 10 -3. It is worth noting that enrichment of iron-sulfur cluster assembly complex and cytochrome complex also helps in the localization of these genes in mitochondrial respiratory machinery [30]. Adjusted p-values of between 1.0 -10 -3 and 1.0 -10 -7 in the molecular function category were found to be highly enriched with electron transfer activity, oxidoreductase activity, NADH dehydrogenase (ubiquinone) activity, and proton transmembrane transporter activity as hub genes. Their involvement in redox-dependent enzymatic activity is further supported by enrichment of iron–sulfur cluster binding [31]. Overall, the extremely low adjusted p-values and high gene ratios collectively confirm that the identified hub genes form a tightly coordinated mitochondrial respiratory module, supporting their central role in cancer-associated metabolic reprogramming.

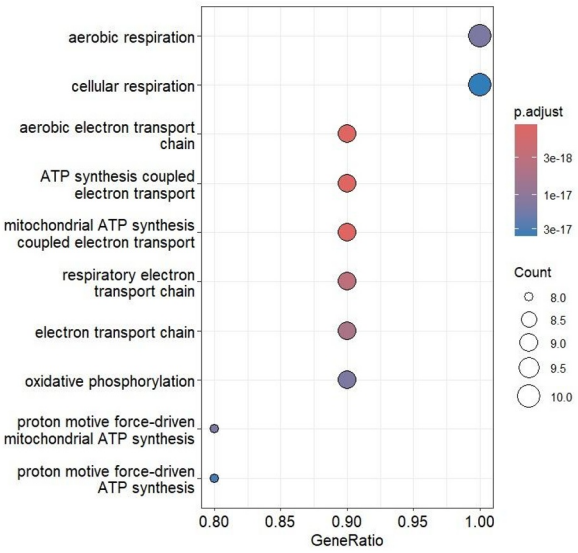

[A]

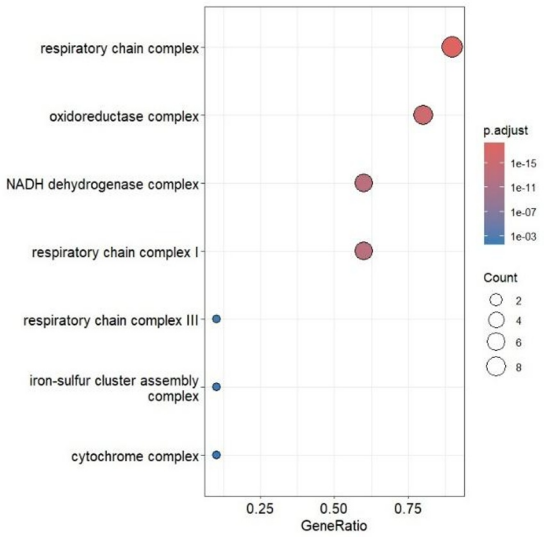

[B]

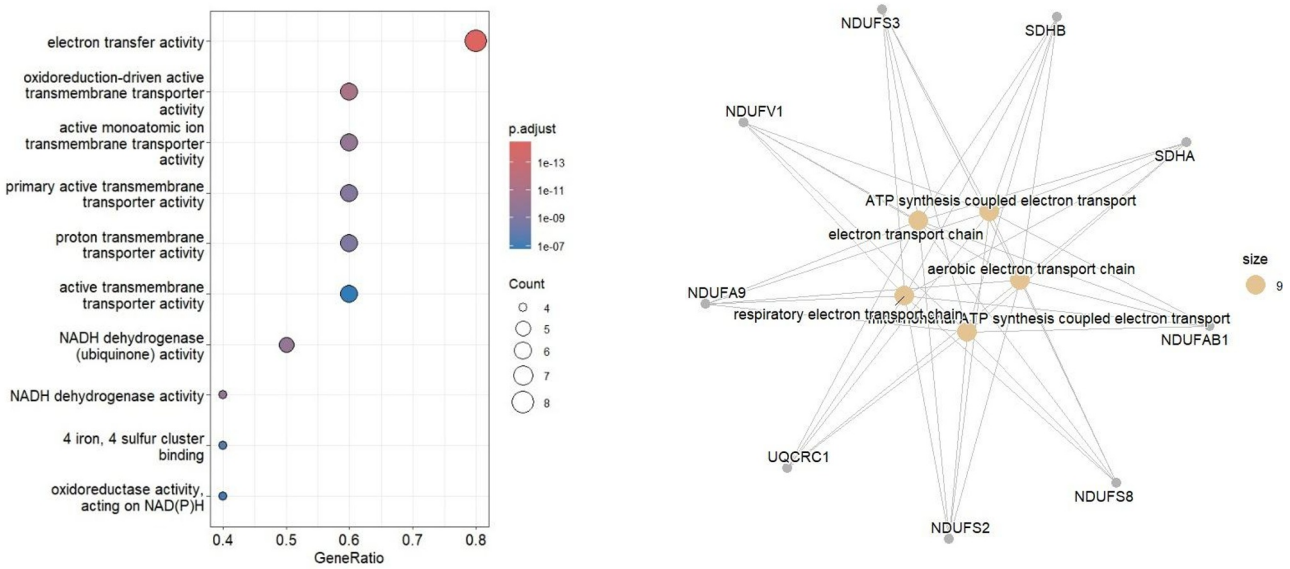

[C] [D]

Fig. 4 (A) GO: Biological Process(B) GO: Cellular Component (C) GO: Molecular Function (D) Gene–ontology (GO) enrichment network visualised using R.

3.3 Dataset Validation

3.3.1 Principal Component Analysis of OXPHOS Hub Genes in Breast and Ovarian Cancer

In this study, tumor and normal samples derived from multiple GEO datasets (GSE10810, GSE14407, GSE18520, GSE29431, and GSE42568), Principal component analysis (PCA) was performed using the expression profiles of OXPHOS hub genes to investigate global transcriptional differences between tumor and normal samples in breast and ovarian cancers. In both datasets, the first two principal components captured a substantial proportion of the total variance, indicating that OXPHOS-associated genes represent a major source of biological variability. During probe-to-gene mapping, NDUFS8 was excluded from downstream expression analyses due to the absence of a corresponding probe on the GPL570 platform, and therefore could not be evaluated in validation datasets.

Together, PC1 and PC2 explained almost 68.7% of the total variation in breast cancer, accounting for 49.3% and 19.4% of the total variance, respectively. Stable OXPHOS gene expression in non-malignant tissue was demonstrated by the comparatively tight cluster formed by normal samples. Tumor samples, on the other hand, showed significant dispersion across all major components, with some overlap between the normal and tumor groups. This pattern indicates varying dependence on mitochondrial oxidative phosphorylation, suggesting significant metabolic variation among breast cancers.

The Ovarian cancer datasets indicated via PCA that the PC1 and PC2 accounted for almost 69.8% of the variance, with PC1 explaining 41% and PC2 explaining 28.8% of the overall variance. The extent of separation of tumor samples and normal samples was consistently and clearly evident down both primary components. Tumor samples grew distinctive and systematized clusters, which is a sign of coordinated transcriptional reorganization of OXPHOS hub genes, whereas normal samples clustered together. The difference between the two key elements leads towards the implication of a number of mitochondrial processes that are involved in causing metabolic differences peculiar to tumors.

As the two types of cancer were compared, significant differences in the OXPHOS-related metabolic activity were observed. Tumor-normal separation was also high with ovarian cancer indicating a more stable and uniform

OXPHOS-dependent metabolic program, whilst breast cancer exhibited partial separation with evidence of widespread tumor dispersion indicating metabolic plasticity and inter-tumor variability. These results suggest that context-dependent and subtype-specific metabolic reprogramming in breast cancer is present but ovarian cancer development is more dominated and homogeneous with mitochondrial oxidative phosphorylation.

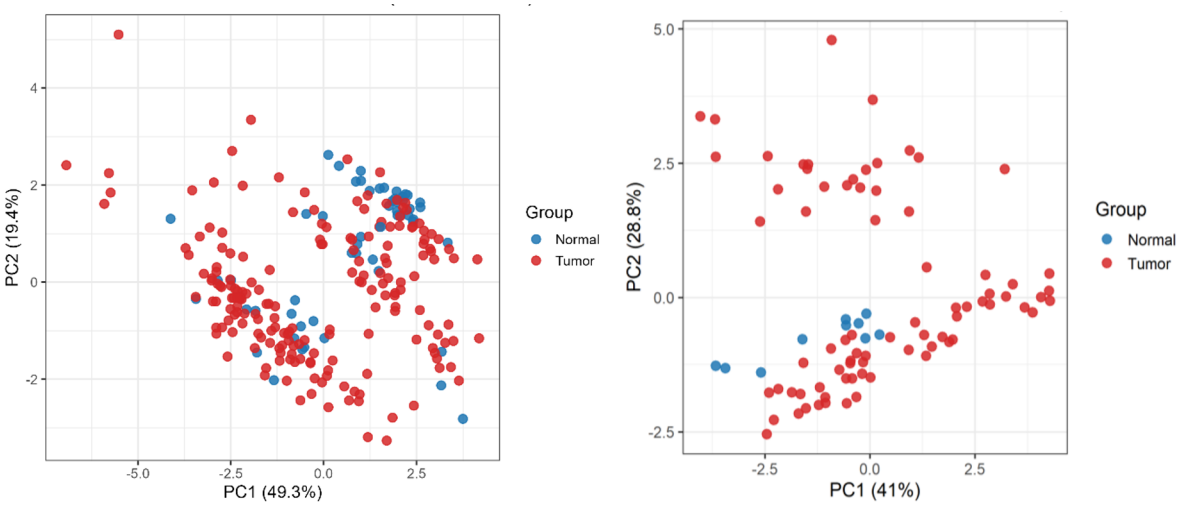

(A) (B)

Fig. 5- Principal component analysis (PCA) of gene expression profiles distinguishing normal and tumor samples. (A) PCA plot for the Breast Cancer dataset showing separation along PC1 (49.3%) and PC2 (19.4%). (B) PCA plot for the Ovarian Cancer dataset showing discrimination along PC1 (41%) and PC2 (28.8%). Blue dots represent normal samples and red dots represent tumor samples, indicating distinct transcriptomic clustering between conditions.

3.3.2 Gene-Gene Correlation in Breast Cancer and Ovarian Cancer (Normal vs Tumor)

A gene-gene correlation study based on samples of normal breast tissue, breast tumor, normal ovarian tissue and ovarian tumor was done to examine the combined role of the mitochondrial oxidative phosphorylation (OXPHOS) genes in breast cancer and ovarian cancer. This investigation was aimed to measure the coordination of OXPHOS genes in normal and malignant states, but not the change of individual gene expression.

The x- and y-axis of the correlation heat maps display the identical set of OXPHOS hub genes, which are the subunits of mitochondrial Complex I (NDUFS2, NDUFA9, NDUFS3, NDUFAB1, NDUFV1), Complex II (SDHA, SDHB), Complex III (UQCRC1), and metabolic reference gene GAPDH. The Pearson correlation coefficient between two genes is plotted in each cell in the heatmap, where the intensity of the color represents the strength of the correlation. Red indicates a strong positive correlation (level of +1), white indicates weak or no correlation (around 0), and blue indicates a strong negative correlation (values below 0). Hierarchical clustering dendrograms group genes with similar patterns of correlation, indicating functional blocks in the network.

The correlation structure in normal breast samples seemed to be rather modular and structured. Specifically, OXPHOS genes from the same mitochondrial complexes showed positive but reasonably balanced associations. While Complex II genes (SDHA and SDHB) formed a strongly linked pair, indicating their known functional reliance, Complex I subunits grouped together with moderate co-expression. Significantly, GAPDH had little association with the majority of mitochondrial genes, suggesting that oxidative phosphorylation and glycolysis function in normal tissue in a regulated and mostly autonomous fashion. All things considered, a well-regulated mitochondrial system with stable but adaptable energy generation is reflected in the normal breast correlation network.

Conversely, there was a strong strengthening and reorganization of gene-gene correlations in the tumor samples of the breast. Most of the OXPHOS gene pairs were associated with high positive correlations, even within the high correlation values, which implies more co-regulation. The Complex I and Complex II genes were more tightly clustered and this indicated a coordinated transcriptional regulation of several elements of the electron

transport chain. It is important to note that GAPDH is more correlated with a number of mitochondrial genes, which indicates metabolic association between glycolysis and OXPHOS in tumor cells. Also, some genes showed a reversal in directionality of correlation relative to normal samples indicating a rewiring of the network and not a general activation of genes.

The comparison between normal and tumor correlation patterns reveals a clear transition from a modular and regulated network in normal tissue to a highly coordinated and tightly interconnected network in breast cancer. This shift suggests that tumor cells reorganize mitochondrial gene interactions to meet increased bioenergetic and biosynthetic demands. individual gene changes collectively result in tumor-specific metabolic phenotypes.

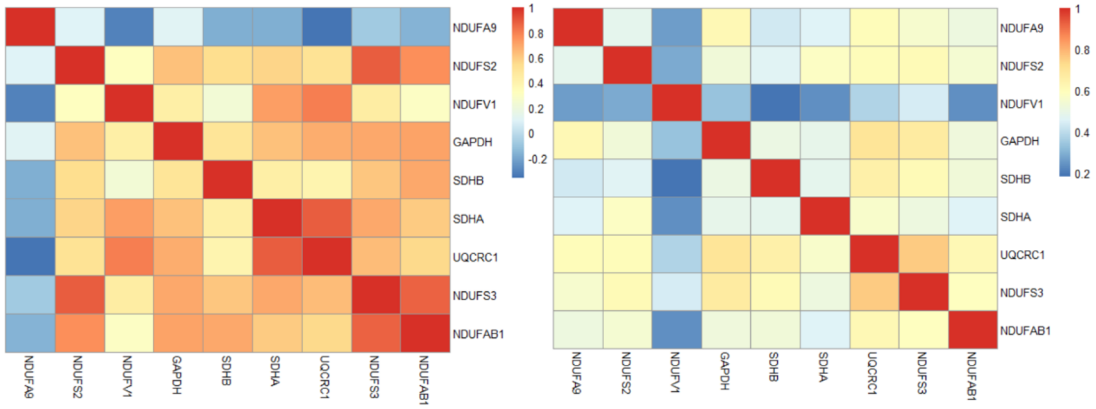

(A) (B)

Fig. 6 Gene–gene correlation heatmaps of selected metabolic hub genes in (A) Breast normal samples and (B) Breast cancer samples. Colour intensity represents the strength and direction of correlation (blue to red scale). Compared to normal tissue, cancer samples exhibit altered correlation patterns, indicating disruption of coordinated metabolic gene regulation in the tumor state.

In contrast, the gene–gene association pattern in normal ovarian samples reveals a modular and balanced mitochondrial structure. The majority of OXPHOS genes show moderately positive relationships, especially when they are part of the same respiratory complex. Normal electron transport chain function is reflected in the clustering of Complex I subunits with coordinated but moderate correlation strengths. Strong mutual connection between the Complex II genes SDHA and SDHB is in line with their required functional interaction. GAPDH and mitochondrial genes have a modest to moderate connection, suggesting that oxidative phosphorylation and glycolysis are still mostly independent in physiological settings. All things considered, this pattern indicates a controlled metabolic state where mitochondrial activity is effectively managed and flexible.

A distinct shift from a flexible, modular mitochondrial network in normal ovarian tissue to a highly coordinated and rewired OXPHOS network in ovarian cancer can be seen when comparing the correlation patterns of normal and malignant tissue. In ovarian cancer, OXPHOS genes function as a cohesive system that is tuned for tumor survival and progression rather than as separate functional units. Overall, the gene–gene correlation analysis reveals that ovarian cancer is characterized by network-level mitochondrial reprogramming, where improved coordination across OXPHOS hub genes defines the tumor metabolic state.

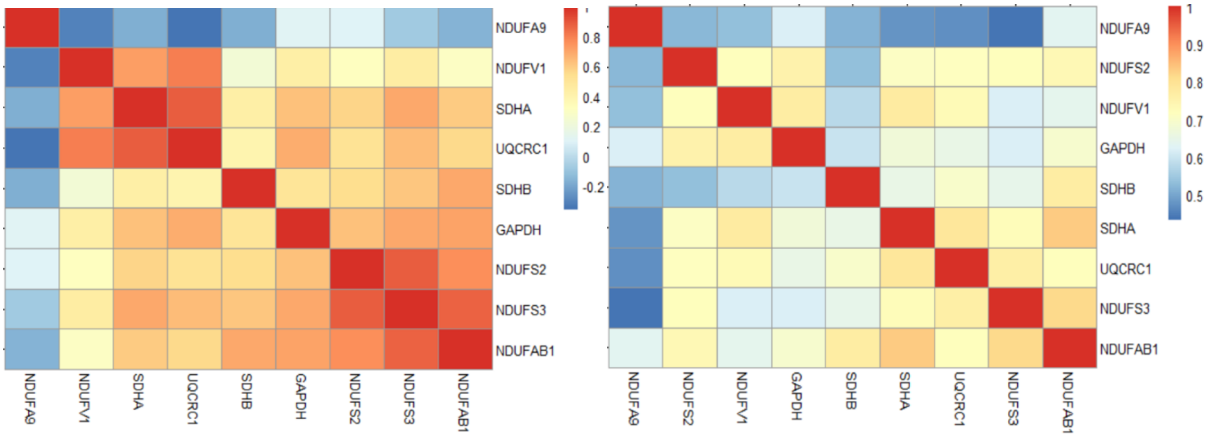

(A) (B)

Fig. 7 Gene–gene correlation heatmaps of selected metabolic hub genes in (A) Ovarian normal samples and (B) Ovarian cancer samples. Colour intensity represents the strength and direction of correlation (blue to red scale). Compared to normal tissue, cancer samples exhibit altered correlation patterns, indicating disruption of coordinated metabolic gene regulation in the tumor state

3.3.3 Correlation Shift Analysis of Mitochondrial Hub Genes in Breast and Ovarian Cancer

The analysis of correlation density distribution demonstrated a specific tumor-related change in co-expression distribution of genes between the mitochondrial hub proteins in both breast and ovarian cancer sets (NDUFS2, NDUFA9, NDUFS3, NDUFAB1, NDUFV1, SDHA, SDHB, and UQCRC1).

Compared with normal tissues, the correlation density of breast cancer tumor samples showed a slight shift to the right, and the tumor curve displayed a more concentrated, sharper peak around moderate-to-high positive correlation value (~0.5–0.6). The normal samples, on the other hand, showed a wider distribution, ranging from lower to higher correlation values. This suggests that the components of Complex I (NDUFS2, NDUFA9, NDUFS3, NDUFAB1, NDUFV1), Complex II (SDHA, SDHB), and Complex III (UQCRC1) exhibit tighter and more coordinated co-expression in breast cancers. Increased regulatory synchronization of oxidative phosphorylation (OXPHOS) genes in malignant tissue is suggested by the tumor density curve's narrowing.

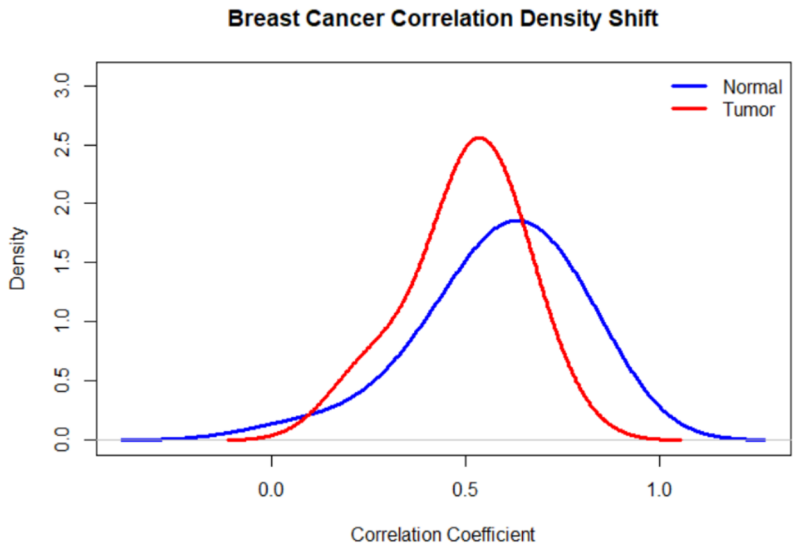

Fig. 8 Correlation density distribution of metabolic hub genes in breast cancer. The density plot compares pairwise correlation coefficients in normal (blue) and tumor (red) samples. A noticeable shift in the distribution indicates altered gene–gene coordination in tumor tissue compared to normal breast tissue.

The correlation shift was particularly noticeable in ovarian cancer. Normal samples displayed a more scattered and larger correlation range, including weaker and even slightly negative correlations, while tumor samples displayed a pronounced rightward displacement and a highly peaked distribution centered at higher positive correlation values (~0.6–0.8). This suggests that the genes involved in the mitochondrial electron transport chain have significantly increased co-expression in ovarian cancers. Increased metabolic integration is shown in the sharper tumor peak, which indicates improved transcriptional coupling of Complex I (NDUF subunits), Complex II (SDHA/SDHB), and Complex III (UQCRC1).

Together, these results show that both cancer types exhibit a tumor-associated increase in coordinated expression of important oxidative phosphorylation hub genes, with ovarian cancer showing a larger correlation shift than breast cancer. The idea of coordinated OXPHOS activation in tumor progression is supported by the elevated co-expression pattern, which indicates metabolic rewiring toward tightly regulated mitochondrial bioenergetics in malignant tissues.

.

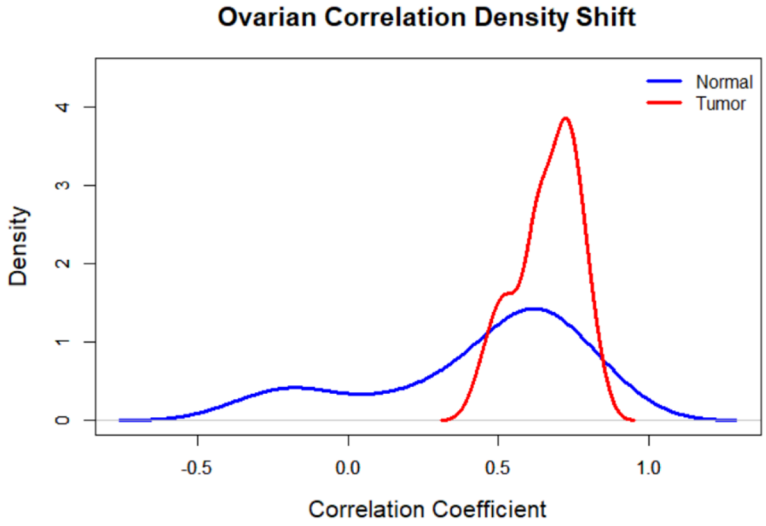

Fig. 9 Correlation density distribution of metabolic hub genes in ovarian cancer. The density curves compare pairwise correlation coefficients in normal (blue) and tumor (red) samples. A distinct shift toward stronger positive correlations in tumor samples indicates altered and potentially tighter gene–gene coordination in ovarian cancer compared to normal ovarian tissue.

3.3.6 Baseline Expression Profile of Mitochondrial Hub Genes

(a) Baseline Log_2-Transformed Expression Levels of Mitochondrial Hub Genes

Log_2-transformed mean expression values were analyzed across normal and tumor samples from ovarian and breast cancer datasets in order to create the baseline transcriptional landscape of mitochondrial hub genes before conducting downstream network studies (Table X). All of the chosen hub genes showed moderate to high levels of expression overall (log_2 values roughly between 7.1 and 12.2), indicating that they were suitable for further correlation, correlation shift, and PCA studies as well as having strong transcriptional activity.

Tumor samples consistently displayed higher expression than normal ovarian tissue for most of the mitochondrial hub genes in the ovarian cancer dataset. Important Complex I subunits, including NDUFA9, NDUFAB1, NDUFS2, NDUFS3, and NDUFV1, showed a discernible increase in tumor samples, with elevations ranging from 0.3 to 1.3 log_2 units. GAPDH expression was also elevated in ovarian tumors, suggesting elevated metabolic activity. When Complex II genes SDHA and SDHB were compared to Complex I components, the former showed relatively minor changes, indicating that their expression was preserved but not considerably altered. This overall

pattern suggests the coordinated activation of genes associated with mitochondrial oxidative phosphorylation in ovarian cancer, which is consistent with an OXPHOS-dependent metabolic state.

Breast cancer samples, on the other hand, showed a more varied expression pattern. Several mitochondrial hub genes exhibited steady or decreased expression in cancers, but GAPDH showed increased expression in tumors compared to normal breast tissue. Interestingly, the mean expression of NDUFA9, NDUFAB1, NDUFS3, NDUFS8, NDUFV1, SDHA, and SDHB was lower in breast tumor samples than in normal breast tissue. The declines were most noticeable for SDHB and NDUFV1. There was just a slight rise in breast cancers in NDUFS2. Both cancer types' UQCRC1 expression was preserved, as evidenced by its relative stability in both normal and malignant samples.

More importantly, these background expression patterns provide essential background data in terms of assessing future gene-gene association, correlation change and PCA analyses, emphasizing that the organization and coordination of network, but not the quantity of expression, is a defining feature of mitochondrial reprogramming in cancer.

Table 2. Log_2-transformed mean expression levels of mitochondrial hub genes in normal and tumor Breast samples

Gene	log2FC	Fold_Change	Adjusted_P_Value	Direction
NDUFV1	-0.2508	0.840400044391814	0.0416380856894716	Downregulated
GAPDH	0.519	1.43358875680531	1.390094909136e-06	Upregulated
NDUFS2	0.364	1.2870071970569	0.0013511156580464	Upregulated
UQCRC1	0.033	1.02292566901164	0.776879295592549	Upregulated
NDUFS3	0.196	1.14363070786225	0.0416380856894716	Upregulated
SDHB	-0.0541	0.963131871835899	0.672270121896404	Downregulated
SDHA	-0.210	0.864258738287094	0.0421697326841823	Downregulated
NDUFA9	0.219	1.16472013583891	0.0416380856894716	Upregulated
NDUFAB1	0.276	1.21136860292996	0.00675952278358849	Upregulated

Table 3. Log_2-transformed mean expression levels of mitochondrial hub genes in normal and tumor Ovarian samples

Gene	log2FC	Fold_Change	Adjusted_P_Value	Direction
NDUFV1	2.568	5.92959078097122	1.41899416411406e-20	Upregulated
GAPDH	1.126	2.18372831038544	1.51369284517888e-06	Upregulated
NDUFS2	0.715	1.64159364391567	0.000244926579906513	Upregulated
UQCRC1	1.367	2.5795786014634	0.000283226092046895	Upregulated
NDUFS3	0.702	1.62723415787484	0.00245900349323505	Upregulated
SDHB	-0.381	0.768041621526848	0.0475133658388717	Downregulated
SDHA	0.454	1.36988746051433	0.0475133658388717	Upregulated
NDUFA9	0.278	1.2123191042942	0.160973607306743	Upregulated
NDUFAB1	-0.113	0.924871817112216	0.670321576247162	Downregulated

b) Differential Expression Analysis of Mitochondrial Hub Genes in Breast and Ovarian Cancer

Differential expression analysis was utilized to quantify tumor–normal transcriptional changes in mitochondrial hub genes across the datasets for breast and ovarian cancer. The x-axis of lollipop plots displays the log_2 fold change (log_2FC) of gene expression between tumor and normal samples; positive values in tumors imply upregulation, whereas negative values suggest downregulation. The vertical dashed line shows that the equation remains unchanged at $log_2FC = 0$. Statistical significance is used to color-code genes, with gray indicating non-

significant changes and red indicating significantly enhanced genes. The y-axis lists the genes that make up the mitochondrial hub.

Out of all the genes examined, GAPDH showed the biggest positive log_2FC in breast cancer, indicating a marked and statistically significant upregulation that is associated with increased glycolytic and metabolic activity in tumor cells. NDUFS2 was significantly upregulated among mitochondrial genes, indicating that particular Complex I components were selectively activated. On the other hand, the majority of other genes linked to OXPHOS, such as NDUFA9, NDUFAB1, NDUFS3, SDHA, SDHB, UQCRC1, and NDUFV1, showed comparatively low log_2FC values and fell short of statistical significance. Interestingly, there was a propensity for both SDHB and NDUFV1 to be downregulated, suggesting that some mitochondrial subunits may be suppressed in breast cancers. Overall, metabolic variability and a partial dependence on mitochondrial pathways are reflected in the limited but selective differential expression shown by the breast cancer DEG profile.

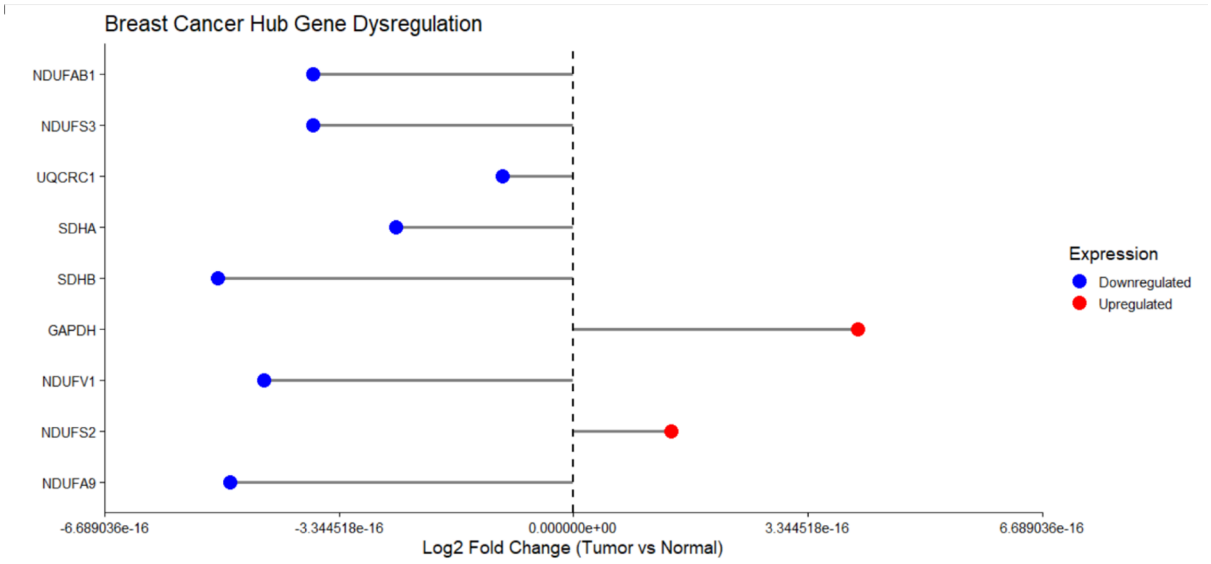

Fig. 10 The lollipop plot shows log_2 fold change (tumor vs. normal) for each gene. Red dots indicate upregulated genes, while blue dots represent downregulated genes in tumor samples. The dashed vertical line at zero denotes no change in expression, highlighting distinct dysregulation patterns of OXPHOS-related hub genes in breast cancer.

A similar but still more evident trend was seen in ovarian cancer. It was indicated again by a substantial and notable increase of GAPDH, and it indicated the existence of high metabolic demand in tumor tissues. Notably, SDHB was downregulated in ovarian tumors, as indicated by a negative log_2 fold change, suggesting potential suppression of specific Complex II components. Although other hub genes in the mitochondrion showed positive log 2FC, most of them were not statistically significant enough to indicate that ovarian cancer did not need the widespread overexpression of certain OXPHOS genes. Rather, small, yet coordinated changes in expression seem to be enough to maintain mitochondrial functioning. SDHB and NDUFV1 had negative log_2FC values meaning that some of the components of the electron transport chain were down regulated.

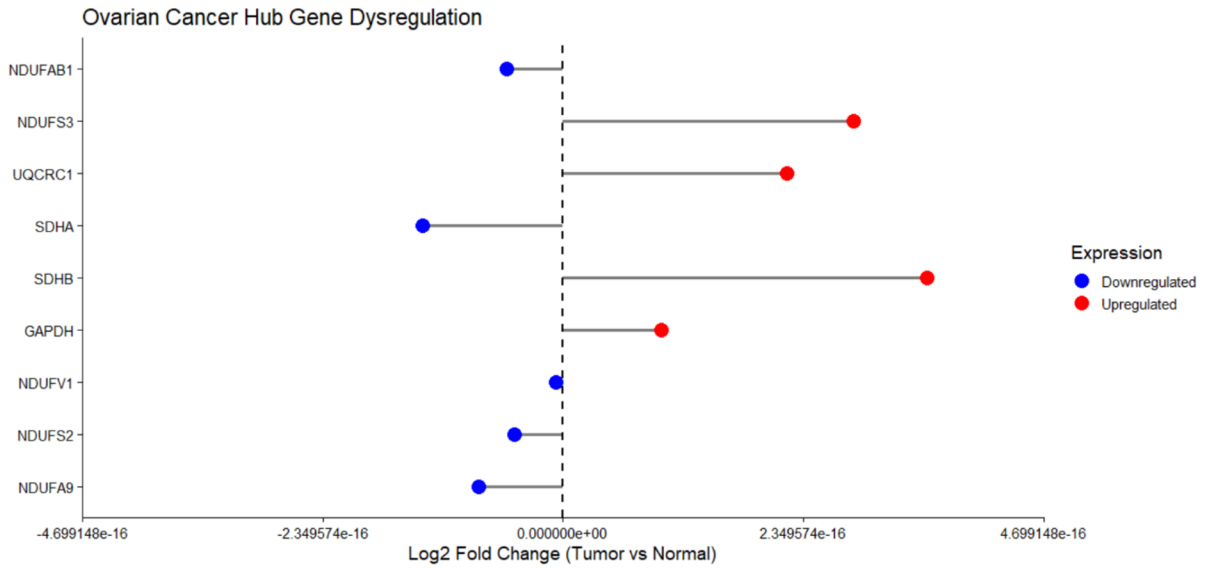

Fig. 11 Differential expression analysis of metabolic hub genes in ovarian cancer. The lollipop plot illustrates $\log_2$ fold change (tumor vs. normal) for each gene, with red dots representing upregulated genes and blue dots indicating downregulated genes in tumor samples. The dashed vertical line at zero denotes no change in expression, highlighting distinct patterns of metabolic gene dysregulation in ovarian cancer.

Different metabolic strategies are revealed by comparing ovarian and breast cancer. While ovarian cancer exhibits more consistent transcriptional trends, especially for genes associated to OXPHOS, breast cancer exhibits diverse and selective dysregulation of mitochondrial genes. Crucially, as demonstrated by the previously presented gene–gene correlation, correlation shift, and PCA analyses, the comparatively weak DEG signals for the majority of mitochondrial hub genes highlight the fact that coordinated network-level regulation, rather than large fold changes in individual genes, is the primary driver of mitochondrial reprogramming in both cancers.

4. Conclusion

Overall, this integrative transcriptome and network-scale study demonstrates that the mitochondrion oxidative phosphorylation hub genes are a functional module which is tightly connected and frequently rewired in ovarian and breast cancers. The metabolic state of the tumor is characterized by reconfiguration at the network level as well as an increased gene-gene interaction despite minor changes in the expression of individual genes in selected cases. Breast cancer exhibits metabolic plasticity, with a selective involvement of mitochondria but ovarian cancer exhibits a stronger and more consistent OXPHOS phenotype. These findings reveal that the main regulator of cancer-related mitochondrial reprogramming is not the dysregulation of a specific gene but rather systems-level coordination.

Altogether, this paper preconditions biomarker-based mitochondrial targeting strategies in solid malignancies and underlines the importance of pathway-based and network-based methods in the detection of metabolic weaknesses.

5. Future Perspectives

However, as much as the study at hand can be used to provide a framework on the network-based metabolic classification of cancer, there are several ways through which these findings can be extended in the future.

To begin with, the combination of transcriptomic data with proteomic and metabolomic data would allow confirming the question of whether transcriptional coordination is reflected in functional changes to metabolic flux. Second, subtype-specific studies in breast cancer (i.e., luminal, HER2-positive, triple-negative) could help understand whether mitochondrial dependence is different among the molecular subgroups. Third, the intra-tumoral heterogeneity in OXPHOS activity could be revealed by incorporating the data on the single-cell transcriptomics.

There is good co-ordination between the genes of Complex I and Complex II to indicate potential susceptibility to the mitochondrial inhibitors such as electron transport chain blockers or electron transport chain blockers like NADH dehydrogenase as a therapeutic consideration. More likely patients could be identified by stratifying patients based on OXPHOS correlation signatures instead of individual-gene expression to determine who would benefit from mitochondrial-targeted medicines.

Finally, implementing this systems-level analytical approach in other metabolically heterogeneous cancers may aid in the creation of precision in oncology targeting tumor bioenergetics.

Acknowledgements: SM and MD acknowledge JIIT, Noida, for providing the entire infrastructure to complete this project.

Author Contributions: Conceptualization, Study supervision, analysis, review and editing: S.M., writing, original draft preparation, analysis: M.D. All authors have read and agreed to the published version of the manuscript.

Competing interests: The authors declare that they have no competing interests.

Funding: Not Applicable

Data Availability: The datasets analyzed during the current study are publicly available in the NCBI Gene Expression Omnibus (GEO) repository under accession numbers GSE10810, GSE42568, GSE29431, GSE14407, and GSE18520.

References

[1] Filho, A.M., Laversanne, M., Ferlay, J., Colombet, M., Piñeros, M., Znaor, A. and Bray, F. (2025). The GLOBOCAN 2022 cancer estimates: Data sources, methods, and a snapshot of the cancer burden worldwide. International Journal of Cancer, 156(7), 1336–1346.

[2] Zhang, R., Siu, M.K., Ngan, H.Y. and Chan, K.K. (2022). Molecular biomarkers for the early detection of ovarian cancer. International Journal of Molecular Sciences, 23(19), 12041.

[3] Sudo, T. (2012). Molecular-targeted therapies for ovarian cancer: Prospects for the future. International Journal of Clinical Oncology, 17, 424–429.

[4] Ohshima, K. and Morii, E. (2021). Metabolic reprogramming of cancer cells during tumor progression and metastasis. Metabolites, 11(1), 28.

[5] Mir, R., Javid, J., Ullah, M.F., Alrdahe, S., Altedlawi, I.A., Mustafa, S.K. and Tayeb, F.J. (2025). Metabolic reprogramming and functional crosstalk within the tumor microenvironment (TME) and a multi-omics anticancer approach. Medical Oncology, 42(9), 373.

[6] Emmings, E., Mullany, S., Chang, Z., Landen Jr, C.N., Linder, S. and Bazzaro, M. (2019). Targeting mitochondria for treatment of chemoresistant ovarian cancer. International Journal of Molecular Sciences, 20(1), 229.

[7] Roth, K.G., Mambetsariev, I., Kulkarni, P. and Salgia, R. (2020). The mitochondrion as an emerging therapeutic target in cancer. Trends in Molecular Medicine, 26(1), 119–134.

[8] Koc, Z.C., Sollars, V.E., Bou Zgheib, N., Rankin, G.O. and Koc, E.C. (2023). Evaluation of mitochondrial biogenesis and ROS generation in high-grade serous ovarian cancer. Frontiers in Oncology, 13, 1129352.

[9] Tomar, M.S., Kumar, A. and Shrivastava, A. (2024). Mitochondrial metabolism as a dynamic regulatory hub to malignant transformation and anti-cancer drug resistance. Biochemical and Biophysical Research Communications, 694, 149382.

[10] Sokolov, D. and Sullivan, L.B. (2025). Mitochondria, OXPHOS, and cancer progression: A modular view. Annual Review of Cancer Biology, 10.

[11] Edgar, R., Domrachev, M. and Lash, A.E. (2002). Gene Expression Omnibus: NCBI gene expression and hybridization array data repository. Nucleic Acids Research, 30(1), 207–210.

[12] Milacic, M., Beavers, D., Conley, P., Gong, C., Gillespie, M., Griss, J., Haw, R., Jassal, B., Matthews, L., May, B., Petryszak, R., Ragueneau, E., Rothfels, K., Sevilla, C., Shamovsky, V., Stephan, R., Tiwari, K., Varusai, T., Weiser, J., Wright, A., Wu, G., Stein, L., Hermjakob, H. and D'Eustachio, P. (2024). The Reactome pathway knowledgebase 2024. Nucleic Acids Research.

[13] Kanehisa, M., Furumichi, M., Sato, Y., Matsuura, Y. and Ishiguro-Watanabe, M. (2025). KEGG: Biological systems database as a model of the real world. Nucleic Acids Research, 53, D672–D677.

[14] Szklarczyk, D., Nastou, K., Koutrouli, M., Kirsch, R., Mehryary, F., Hachilif, R., Hu, D., Peluso, M.E., Huang, Q., Fang, T., Doncheva, N.T., Pyysalo, S., Bork, P., Jensen, L.J. and von Mering, C. (2025). The STRING database in 2025: protein networks with directionality of regulation. *Nucleic Acids Research*, 53(D1), D730–D737.

[15] Shannon, P., Markiel, A., Ozier, O., Baliga, N.S., Wang, J.T., Ramage, D., Amin, N., Schwikowski, B. and Ideker, T. (2003). Cytoscape: A software environment for integrated models of biomolecular interaction networks. Genome Research, 13(11), 2498–2504.

[16] Reimand, J., Kull, M., Peterson, H., Hansen, J. and Vilo, J. (2007). g: Profiler—A web-based toolset for functional profiling of gene lists from large-scale experiments. Nucleic Acids Research, 35(Web Server issue), W193.

[17] Sherman, B.T., Hao, M., Qiu, J., Jiao, X., Baseler, M.W., Lane, H.C., Imamichi, T. and Chang, W. (2022). DAVID: A web server for functional enrichment analysis and functional annotation of gene lists (2021 update). Nucleic Acids Research, 50(W1), W216–W221.

[18] Ge, S.X., Jung, D. and Yao, R. (2020). ShinyGO: A graphical gene-set enrichment tool for animals and plants. Bioinformatics, 36(8), 2628–2629.

[19] Hirst, J. (2013). Mitochondrial complex I. Annual Review of Biochemistry, 82(1), 551–575.

[20] Sazanov, L.A. (2015). A giant molecular proton pump: Structure and mechanism of respiratory complex I. Nature Reviews Molecular Cell Biology, 16(6), 375–388.

[21] Vinothkumar, K.R., Zhu, J. and Hirst, J. (2014). Architecture of mammalian respiratory complex I. Nature, 515(7525), 80–84.

[22] Rutter, J., Winge, D.R. and Schiffman, J.D. (2010). Succinate dehydrogenase—Assembly, regulation and role in human disease. Mitochondrion, 10(4), 393–401.

[23] Brière, J.J., Favier, J., Ghouzzi, V.E., Djouadi, F., Bénit, P., Gimenez, A.P. and Rustin, P. (2005). Succinate dehydrogenase deficiency in human. Cellular and Molecular Life Sciences, 62(19), 2317–2324.

[24] Yu, C.A., Xia, D., Kim, H., Deisenhofer, J., Zhang, L., Kachurin, A.M. and Yu, L. (1998). Structural basis of functions of the mitochondrial cytochrome bc1 complex. Biochimica et Biophysica Acta - Bioenergetics, 1365(1-2), 151–158.

[25] Chen, Q., Vazquez, E.J., Moghaddas, S., Hoppel, C.L. and Lesnefsky, E.J. (2003). Production of reactive oxygen species by mitochondria: Central role of complex III. Journal of Biological Chemistry, 278(38), 36027–36031.

[26] Liberti, M.V. and Locasale, J.W. (2016). The Warburg effect: How does it benefit cancer cells? Trends in Biochemical Sciences, 41(3), 211–218.

[27] Sirover, M.A. (2011). On the functional diversity of glyceraldehyde-3-phosphate dehydrogenase: Biochemical mechanisms and regulatory control. Biochimica et Biophysica Acta - General Subjects, 1810(8), 741–751.

[28] Sorgato, M.C., Lippe, G., Seren, S. and Ferguson, S.J. (1985). Partial uncoupling or inhibition of electron transport rate have equivalent effects on the relationship between the rate of ATP synthesis and proton-motive force in submitochondrial particles. FEBS Letters, 181(2), 323–327.

[29] Bagkos, G., Koufopoulos, K. and Piperi, C. (2014). ATP synthesis revisited: New avenues for the management of mitochondrial diseases. Current Pharmaceutical Design, 20(28), 4570–4579.

[30] Xu, X.M. and Møller, S.G. (2011). Iron–sulfur clusters: Biogenesis, molecular mechanisms, and their functional significance. Antioxidants & Redox Signaling, 15(1), 271–307.

[31] Stiban, J., So, M. and Kaguni, L.S. (2016). Iron-sulfur clusters in mitochondrial metabolism: Multifaceted roles of a simple cofactor. Biochemistry (Moscow), 81(10), 1066–1080.